Catalysis Today 147 (2009) 77–85

Contents lists available at ScienceDirect

Catalysis Today

journal homepage: www.elsevier.com/locate/cattod

Catalytic conversion of cellulose into ethylene glycol over supported carbide catalysts

Na Ji [a,b], Tao Zhang [a,*], Mingyuan Zheng [a], Aiqin Wang [a], Hui Wang [a,b], Xiaodong Wang [a], Yuying Shu [a], Alan L. Stottlemyer [c], Jingguang G. Chen [c,**]

[a] *State Key Laboratory of Catalysis, Dalian Institute of Chemical Physics, Chinese Academy of Sciences(CAS), Dalian 116023, China*
[b] *Graduate School of the Chinese Academy of Sciences, Beijing 100049, China*
[c] *Department of Chemical Engineering, Center for Catalytic Science and Technology (CCST), University of Delaware, Newark, DE 19716, USA*

ARTICLE INFO

Article history:
Available online 17 April 2009

Keywords:
Biofuels
Catalysis
Cellulose
Sustainable chemistry
Tungsten carbides

ABSTRACT

In the current paper we present a combined catalytic and surface science studies to evaluate the utilization of carbide catalysts for the conversion of cellulose to polyols, especially to ethylene glycol (EG). Based on catalytic studies over a W_2C catalyst, the EG yield has been optimized by varying H_2 pressure, reaction temperature and time. The catalytic performance has been compared for several types of supported catalysts, including tungsten carbides, molybdenum carbides and platinum on different supports. Among all the catalysts, tungsten carbide supported on activated carbon, W_2C/AC, shows the highest EG yield, which is further enhanced to 61% with the promotion of Ni. The corresponding surface science studies indicate that the enhanced EG yield is at least partially due to a weaker bonding between EG and Ni-promoted tungsten carbide surface.

1. Introduction

Cellulose is the most abundant source of biomass [1,2]. Since it comes mainly from grass and agricultural and wood waste, the industrial utilization of cellulose would avoid potential competition with the food supply. Thus far, the conversion of cellulose into fuels and industrially important chemicals has been regarded as one of the most promising approaches to sustainable energy production. The utilization of cellulose can be generally divided into two steps. In the first step, cellulose is selectively hydrolyzed into glucose; and in the second step, the glucose can be further converted into fuels and chemicals. However, unlike other water soluble polysaccharides, cellulose has a highly crystalline structure composed of β-1, 4-glycosidic bonds of D-glucose and is therefore difficult to hydrolyze [3–6]. Up to now, the hydrolysis of cellulose with enzymes [7], mineral acids [8], base [9] or supercritical water [10] still suffers from a series of problems such as separation of products and catalysts, corrosion hazards, as well as control of enzymes. Ideally, it is preferred to convert cellulose into fuels or chemicals in a single-step catalytic process. For such a one-step process, one of the main challenges is to search for a suitable catalyst that is able to promote several types of reactions including hydrolysis, hydrogenolysis, and hydrogenation. A representative example toward this direction is the one-step catalytic conversion of cellulose into polyols, which was first developed by Fukuoka et al. [11]. Using Pt/Al_2O_3 as the catalyst, they obtained sugar alcohols with a 31% yield (25% sorbitol and 6% mannitol). Nevertheless, in their reaction conditions, the cellulose conversion rate was not very high. Following Fukuoka's work, Luo et al. further studied this reaction [12]. By elevating the reaction temperature and using Ru/AC as the catalyst, they greatly increased the cellulose conversion and the yield of sugar alcohols. However, a drawback in the above two studies is the use of precious metal catalysts. It is noted that the precious metal amount is relatively high, reaching 4–10 mg per gram of cellulose. This is obviously too expensive for processing large quantities of cellulose. It is therefore highly desirable to develop a less expensive but efficient catalyst for cellulose conversion.

Recently, we reported that Ni-promoted W_2C catalyst could be a promising substitute for precious metal catalyst in cellulose conversion [13]. It is well known that transition metal carbides have similar properties to Pt-group metals for a wide variety of reactions [14–22]. One distinguished feature of the W_2C catalyst from Pt or Ru catalysts in this reaction is its unique high selectivity to ethylene glycol [13]. Currently EG is produced mainly from ethylene via the intermediate ethylene oxide in the petrochemical industry. The global production of EG in 2007 is estimated to be 17.8 million tonnes, up by 5.4% from 2006 [23]. In view of the importance and increasing demand of EG in the plastics industry

---

* Corresponding author. Tel.: +86 411 8437 9015; fax: +86 411 8468 5940.
** Corresponding author. Tel.: +1 302 831 0642; fax: +1 302 831 2085.
E-mail addresses: taozhang@dicp.ac.cn (T. Zhang), jgchen@udel.edu (J.G. Chen).

0920-5861/$ – see front matter © 2009 Elsevier B.V. All rights reserved.
doi:10.1016/j.cattod.2009.03.012

for the manufacture of polyester fibers and resins, and in the automotive industry as an antifreeze, its production directly from cellulose will open a new way for reducing dependence on petroleum.

In the present paper, we will give a more detailed description of the carbide catalyzed cellulose conversion, including the effects of reaction conditions and catalyst compositions on the product distribution, the recyclability of the catalyst, and the promoting effect of Ni on the carbide catalysts.

2. Experimental

2.1. Pretreatment of carbon supports

Several commercial carbon materials were used as the supports for the carbide catalysts, including activated carbon (AC, NORIT Company, Netherland, surface area 709 m^2/g), carbon black (CB, Vulcan XC-72R, Cabot Company, USA, surface area 186 m^2/g), and activated carbon fiber (ACF, Anshan AC company, China, surface area 358 m^2/g). In order to exclude any possible influences by the impurity metals on the commercial carbon supports, all the carbon supports were treated with nitric acid solution (33 wt%) at 353 K for 24 h prior to the deposition of active metal component.

2.2. Catalyst preparation

The carbon supported tungsten carbide (W_2C) catalysts were prepared by carbothermal hydrogen reduction (CHR) method according to our previous report [24]. In detail, the carbon support was impregnated with an aqueous solution of ammonium metatungstate (AMT) by an incipient wetness method, and dried at 393 K for 12 h. The resultant precursor was then carburized in a hydrogen flow by a three-stage heating ramp: from room temperature (RT) to 723 K at 10 K/min, then to 1073 K at 1 K/min, followed by holding at 1073 K for 1 h. Prior to exposure to air, the as-prepared carbide catalyst was passivated in a flow of 1% O_2/N_2 for 12 h at RT. The nominal weight loading of tungsten was 30%.

The Ni-promoted W_2C/AC catalysts were prepared with the similar procedure as above, except that the catalyst precursor was obtained by incipient wetness impregnation with a mixture solution containing AMT and nickel nitrate [25]. The nominal weight loadings of nickel were varied from 1% to 3%. The resultant catalysts are denoted as Ni-W_2C/AC-X, where X represents the CHR temperature.

When alumina was used as the support, the preparation procedure was slightly different from the above described. The γ-Al_2O_3 support (home made, surface area 198 m^2/g) was impregnated with AMT or a mixture of AMT and nickel nitrate, followed by drying at 393 K for 12 h and calcining at 773 K in air for 3 h to obtain WO_3/γ-Al_2O_3 or NiO-WO_3/γ-Al_2O_3 precursor. The precursor was then carburized at 1123 K in 20% CH_4/H_2 for 1 h. The passivation procedure was the same as described above. The resultant catalyst is denoted as WC_x/Al_2O_3-1123 or Ni-W_2C/Al_2O_3-1123, where 1123 represents the carburization temperature.

In a similar procedure, a series of supported molybdenum carbide (Mo_2C) catalysts were also prepared, and denoted as Mo_2C/AC-973, Mo_2C/Al_2O_3-973, Ni-Mo_2C/AC-973, and Ni-Mo_2C/Al_2O_3-973, respectively. For comparison, Pt/γ-Al_2O_3, Pt/AC, and Ni/AC were prepared by an incipient wetness impregnation method. The samples were calcined at 723 K (in air for Pt/γ-Al_2O_3 and in N_2 for the other two catalysts) for 3 h and reduced in H_2 at 673 K for 1 h. The Pt loading was 2.5 wt% and Ni loading was 2 wt%.

2.3. Characterization method

Powder X-ray diffraction (XRD) patterns of the samples were obtained with an X′ pert (PANalytical) diffractometer operated at 40 kV and 100 mA, using Ni-filtered Cu-Kα radiation. Transmission electron microscopy (TEM) analysis was performed on a JEM-2000EX (JEOL) microscope.

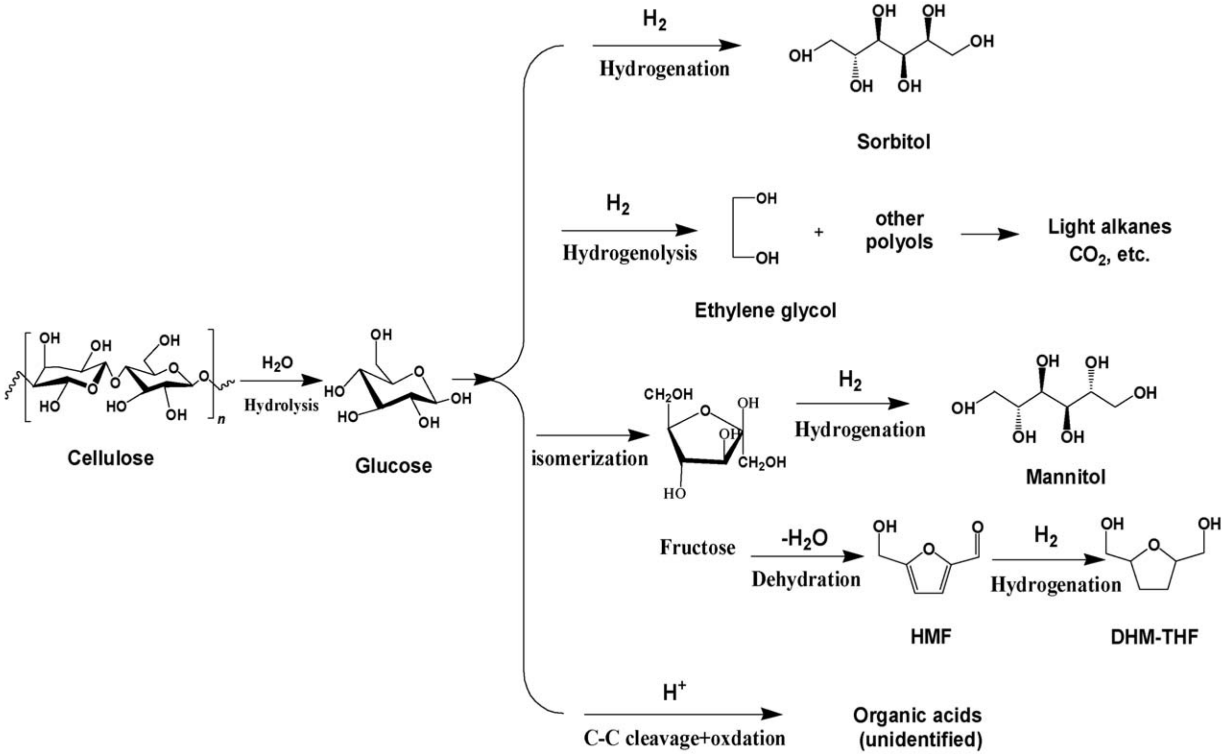

Scheme 1. Possible reactions for the conversion of cellulose.

Microcalorimetry of CO adsorption was performed at 313 K using a Calvet-type microcalorimeter (Setaram BT 2.15) as described in detail elsewhere to determine the CO uptake and to calculate dispersion of active sites [26], the dispersion was calculated from the CO chemisorption amount with the differential heat greater than 40 kJ/mol on each catalyst. N_2 adsorption–desorption experiments were performed with a micromeritics model ASAP 2010 surface area analyzer. The specific surface areas of samples were determined using the Brunauer–Emmett–Teller (BET) method. The pore volume and pore size distribution were derived from the desorption profiles of the isotherms using the Barrett–Joyner–Halanda (BJH) method.

Temperature-programmed reduction of H_2 (H_2-TPR) experiment was performed with a micromeritics Autochem 2920 chemisorber. Prior to the measurement, the catalyst sample was pretreated in Ar at 393 K for 2 h to remove adsorbed water. After cooling to RT in Ar, the gas flow was switched to 10% H_2 in Ar and the sample was heated from RT to 1173 K with a temperature ramp of 10 K/min. Mass spectrometry was used to monitor the CH_4 signal.

Inductively coupled plasma (ICP) experiments were performed on a Thermo IRIS Intrepid II spectrum apparatus to test the actual Ni loadings of the catalysts and the metal concentration in the liquid-phase products.

2.4. Catalyst evaluation

The catalytic conversion of cellulose (Merck, microcrystalline with an average particle size of ~90 μm and a specific surface area of 1.7 m^2/g) was carried out in a stainless-steel autoclave (Parr Instrument Company, 100 ml) typically at 6 MPa H_2 pressure (measured at RT) and at 518 K for 30 min. For each reaction, 0.5 g cellulose, 0.15 g catalyst and 50 ml water were put into the reactor, and stirred at a rate of 1000 rotations/min. After the reaction, the liquid-phase products were analyzed by HPLC and ESI-MS. Cellulose conversions were determined by the change of cellulose weight before and after the reaction, and denoted as $\text{Conversion}_{\text{WT}}$. Alternatively, they were also calculated based on the TOC (total organic carbons) analysis of the liquid product, according to the following equation:

$$\text{Conversion}_{\text{TOC}} = \frac{\text{TOC}}{4230} \times 100\%,$$

where TOC (in the unit of ppm) refers to the total organic carbon in the liquid product, and 4230 (ppm) refers to the carbon content of the cellulose fed in the reactor which was obtained by elemental analysis. The difference between the two conversions is tentatively regarded as the amount of carbon-containing gas produced from cellulose degradation. It should be pointed out that when the conversions of cellulose were calculated based on the TC (total carbons, include both organic and inorganic carbons) rather than the TOC of the liquid product, they are very close to the $\text{Conversion}_{\text{WT}}$ (the difference smaller than 5%), implying that a portion of CO_2 gas produced by cellulose degradation has entered into the liquid phase by reacting with H_2O. The analysis on the gas product confirms that it mainly contains CO_2 and CH_4. The yield of polyols was calculated by the equation:

$$\text{Yield}\,(\%) = \frac{(\text{weight of polyol in the products})}{(\text{weight of cellulose put into the reactor})} \times 100\%.$$

2.5. Surface science studies

The ultra-high vacuum (UHV) system used for surface science studies has been described previously [27]. Briefly, it is a three-level stainless-steel chamber equipped with Auger electron spectroscopy (AES) for analysis of surface compositions and high-resolution electron energy loss spectroscopy (HREELS) for vibrational studies of surface intermediates. A polycrystalline tungsten foil (Alfa Aesar, 99.95%) was spot welded to two tantalum posts that served both as thermal contacts for liquid nitrogen cooling and electrical connections for resistive heating. In this manner, the sample could be cooled to 90 K and heated to 1100 K. The procedure for the synthesis of tungsten carbide (WC) from the tungsten foil has been described previously [28]. The deposition of submonolayer coverage of Ni on WC, as verified by AES, was carried out at 300 K using physical vapor deposition (PVD) [29]. The WC or Ni/WC sample was exposed to 2 L (1 L = 1 × 10^{-6} torr s) ethylene glycol at 200 K. HREELS spectra were recorded after the surface

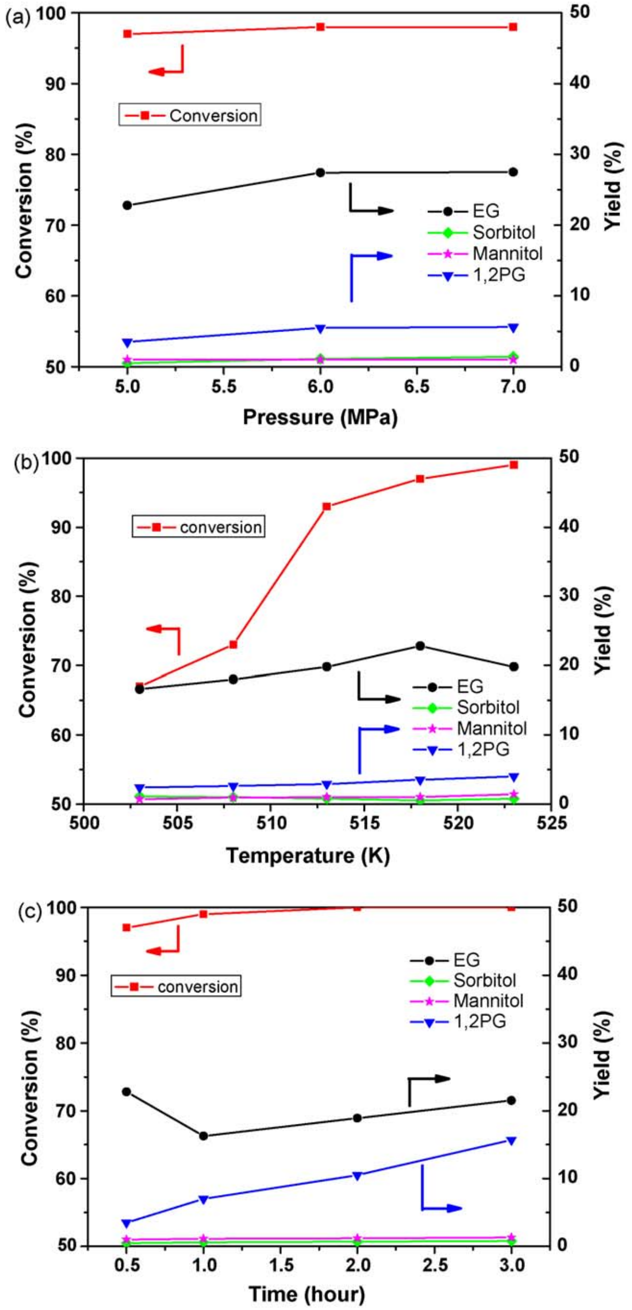

Fig. 1. Effect of reaction conditions on the conversion of cellulose and yield of main products over W_2C/AC-1073 catalyst. (a) Effect of H_2 initial pressure. Reaction temperature = 518 K; reaction time = 30 min; (b) effect of reaction temperature. H_2 initial pressure = 6 MPa; reaction time = 30 min; (c) effect of reaction time. H_2 initial pressure = 6 MPa; reaction temperature = 518 K.

Table 1

Cellulose conversion and polyol yields over different catalysts at 518 K and 6 MPa for 30 min.

Entry	Catalyst[a]	$Conversion_{WT}$ (%)[b]	$Conversion_{TOC}$ (%)	$Conversion_{TC}$ (%)	Gas_{TOC} (%)	Yield (%)[c]				
						Ethylene glycol	Sorbitol	Mannitol	Erythritol	1,2 Propylene glycol
1	Pt/AC	66	56	61	10	8.2	3.2	1.5	1.0	5.9
2	Ni/AC	68	55	61	13	5.2	3.1	1.6	0.7	4.3
3	W_2C/AC-1073	98	87	95	11	27.4	1.1	1.0	0.6	5.5
4	WC_x/AC-1123	97	83	89	14	25.4	0.9	0.9	0.5	4.9
5	Mo_2C/AC-973	85	74	79	11	5.3	0.9	0.5	0.2	2.8
6	Pt/Al_2O_3	98	89	95	9	14.2	9.5	6.0	1.7	9.3
7	WC_x/Al_2O_3-1123	95	71	87	24	3.4	0.8	0.8	0.1	1.1
8	Mo_2C/Al_2O_3-973	80	69	75	11	3.4	0.8	0.2	0.2	0.5
9	W_2C/CB-1073	98	87	95	11	18.9	0.4	0.5	0.6	4.4
10	W_2C/ACF-1073	85	73	79	12	5.3	0.2	0.2	0.2	1.0
11	1%Ni-W_2C/AC-973	98	90	95	8	52.1	3.2	2.1	2.2	7.7
12	2%Ni-W_2C/AC-973	100	93	99	7	61.0	3.9	1.9	2.3	7.6
13	3%Ni-W_2C/AC-973	95	88	94	7	49.8	4.7	1.5	2.6	4.3
14	1%Ni-W_2C/AC-1073	90	82	87	8	36.1	10.4	2.6	2.5	4.3
15	2%Ni-W_2C/AC-1073	92	83	87	9	39.2	10.9	2.7	2.5	4.4
16	3%Ni-W_2C/AC-1073	86	78	83	8	33.8	11.3	2.8	2.5	4.5
17	2%Ni-W_2C/Al_2O_3-1123	95	83	88	12	5.8	0.3	0.2	0.2	3.8
18	2%Ni-Mo_2C/AC-973	87	72	78	15	11.3	4.1	2.7	1.1	5.1
19	2%Ni-Mo_2C/AC-873	80	60	72	20	7.2	0.4	0.3	8.3	4.7
20	2%Ni-Mo_2C/Al_2O_3-973	82	61	73	21	7.2	1.5	0.5	0.2	4.5
21	2%Ni-Mo_2C/Al_2O_3-873	80	66	72	14	6.7	1.4	0.3	0.2	4.5
22	W_2C/AC-1073-2[d]	98	89	97	9	23.6	0.6	0.6	0.6	2.8
23	W_2C/AC-1073-3[e]	98	91	97	7	22.5	0.6	0.6	0.6	2.8
24	2%Ni-W_2C/AC-973-2[f]	100	92	98	8	56.0	5.4	3.4	1.3	6.7
25	2%Ni-W_2C/AC-973-3[g]	100	92	98	8	51.0	5.4	3.4	1.3	6.7

[a] The metal loadings (wt%) are referred to nominal values, W loading = 30 wt%, Mo loading = 30 wt%, and Pt loading = 2.5 wt%.

[b] The conversion was calculated by the weight difference of cellulose before and after reaction with an uncertainty of ±3%.

[c] The yield of polyols was calculated by the equation: yield (%) = (weight of polyol in the products)/(weight of cellulose put into the reactor) × 100%.

[d] W_2C/AC-1073 K in the second run.

[e] W_2C/AC-1073 K in the third run.

[f] 2%Ni-W_2C/AC-973 in the second run.

[g] 2%Ni-W_2C/AC-973 in the third run.

was heated to higher temperatures and allowed to cool down to 100 K.

3. Results and discussion

The direct conversion of cellulose into polyols is a rather complex process, involving hydrolysis of cellulose to glucose, hydrogenation of glucose to hexitol (sorbitol and mannitol), hydrogenolysis of glucose to low-molecular polyols such as ethylene glycol, propylene glycol and glycerol, as well as further degradation of polyols to gas products, such as CO, CO_2, H_2 and alkanes. The possible reactions are summarized in Scheme 1. To achieve a high selectivity to the desired product, e.g., ethylene glycol, the optimization of reaction conditions and the choice of a suitable catalyst prove to be very important. In the present work, we firstly investigated the effect of reaction conditions such as pressure, reaction temperature and time, on the catalytic performance of W_2C/AC catalyst. Under these optimized conditions, we then compared a series of non-noble metal catalysts for the direct conversion of cellulose to ethylene glycol.

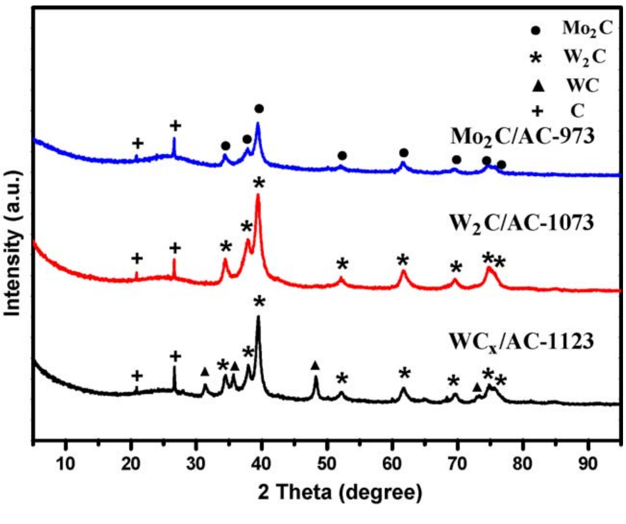

Fig. 2. XRD patterns of W_2C/AC-1073, WC_x/AC-1123 and Mo_2C/AC-973.

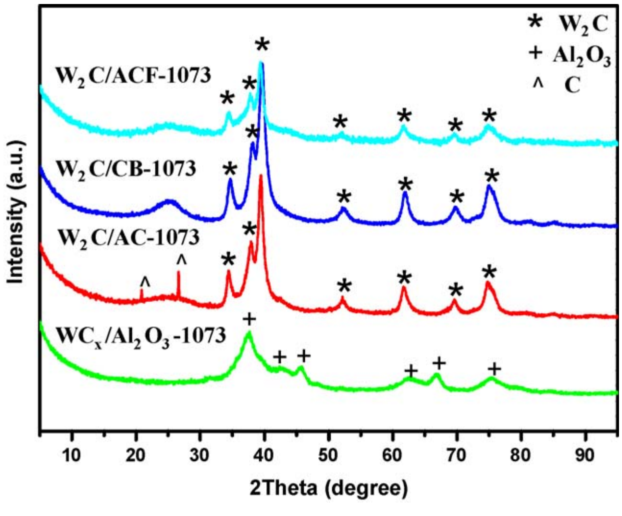

Fig. 3. XRD patterns of W_2C/ACF-1073, W_2C/CB-1073, W_2C/AC-1073, and WC_x/Al_2O_3-1123.

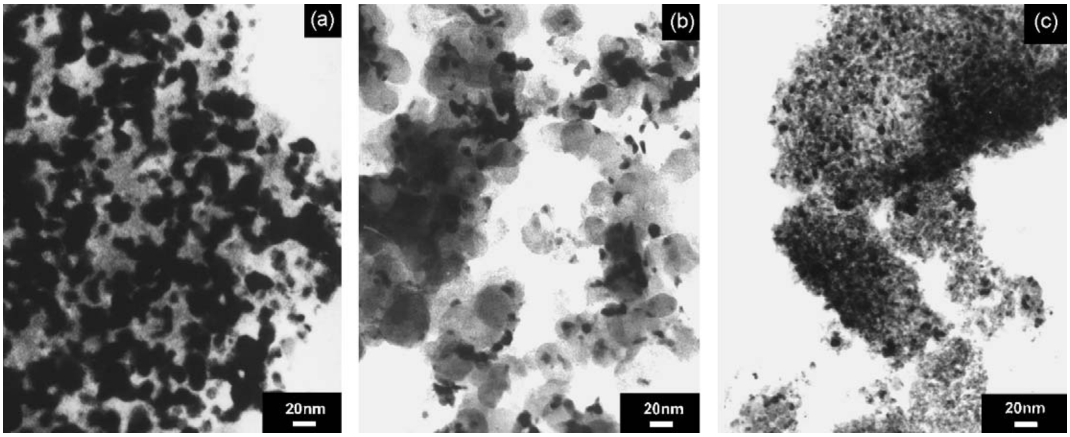

Fig. 4. TEM images of (a) W_2C/AC-1073; (b) W_2C/CB-1073; and (c) WC_x/Al_2O_3-1123.

3.1. *Optimization of reaction conditions*

The effect of reaction conditions on the conversion of cellulose and the yield of EG was investigated on the W_2C/AC-1073 catalyst. As shown in Fig. 1, keeping the reaction temperature at 518 K and reaction time at 30 min, increasing the initial H_2 pressure from 5 MPa to 6 MPa led to a slight increase in the EG yield and cellulose conversion. Further increasing the H_2 pressure from 6 MPa to 7 MPa, the EG yield remained almost unchanged. Based on this observation, we choose 6 MPa as the optimal H_2 pressure. Quite different from the influence of pressure, it is found that the product distribution is sensitive to the changes in reaction temperature and time. With an increase in the reaction temperature from 503 K to 523 K, the EG yield exhibited a gradual increase until its maximum value at 518 K, and then decreased at a higher reaction temperature. On the contrary, the cellulose conversion increased monotonously with the reaction temperature. This result suggests that the formation of EG is not a thermally stable process, with EG undergoing further decomposition into smaller molecules at a higher reaction temperature. Similarly, the EG yield was greatest after 0.5 h. However, it shows an unusual valley at 1 h, and then increases with prolonging the reaction time. It is noted that the yield of 1,2-propylene glycol (1,2 PG) increased rapidly with the reaction time, and it was as high as 16% at 3 h. It is known that the 1,2-propylene glycol is widely used as materials of resin, plasticizer, surfactant, emulsifier and anti-emulsifier, and also antifreeze and heat carrier [30]. Thus, by optimizing the reaction conditions, it is possible to obtain high yields of both EG and 1,2-propylene glycol over the tungsten carbide catalysts. In the present work, we focus only on the enhancement of EG yield, for which the optimized conditions were determined as: reaction temperature of 518 K, reaction time of 0.5 h, and initial H_2 pressure of 6 MPa.

3.2. *Effect of active phase on the catalytic conversion of cellulose*

As shown in Table 1, when the active component on the AC support was compared for Pt, Ni and carbides, a remarkable difference in the product selectivity can be observed. Both the Pt/AC and Ni/AC catalysts exhibited a moderate conversion of cellulose (66–68%) and a low yield of EG (less than 10%). In contrast, the AC supported tungsten carbide catalysts led to a nearly complete conversion of cellulose. Moreover, EG predominates over the other polyols in the products, with the yield as high as 27.4% over the W_2C/AC-1073 catalyst. Note that the W_2C/AC-1073 catalyst is slightly more active and selective towards EG than

Table 2
The dispersion of active sites on different supported catalysts based on CO uptake.

Catalysts	W_2C/AC-1073	W_2C/ACF-1073	W_2C/CB-1073	WC_x/Al_2O_3-1123
Dispersion (%)	5.5	6.3	2.3	8.0

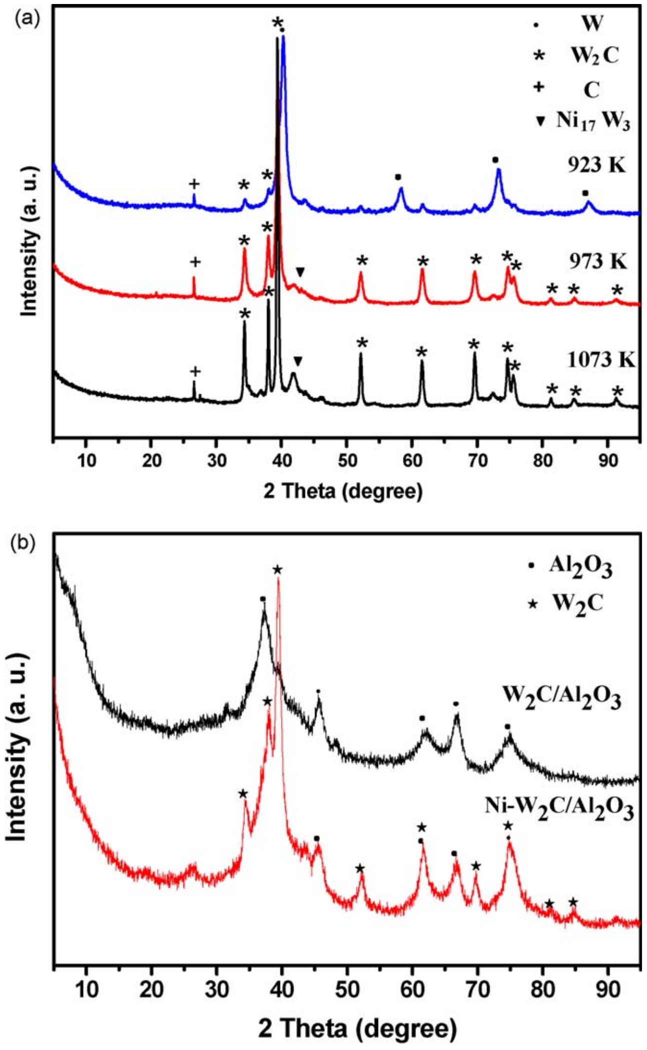

Fig. 5. XRD patterns of (a) 2%Ni-W_2C/AC catalysts prepared at different carbothermal hydrogen reduction temperatures and (b) 2%Ni-W_2C/Al_2O_3 as well as W_2C/Al_2O_3 prepared at 1123 K.

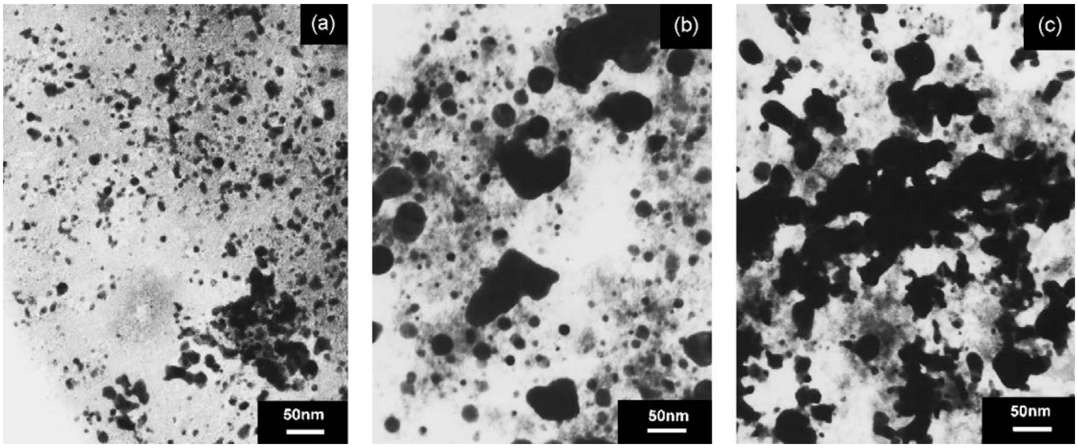

Fig. 6. TEM images of (a) W_2C/AC-1073; (b) 2%Ni-W_2C/AC-973; and (c) 2%Ni-W_2C/AC-1073.

the WC_x/AC-1123. From the XRD patterns in Fig. 2, one can see that the W_2C/AC-1073 catalyst has a single active phase W_2C, while the WC_x/AC-1123 catalyst presents a mixture phase composed of W_2C and WC. The only difference in preparing the two catalysts is the CHR temperature. Clearly, a higher CHR temperature promoted further carburization of W_2C to form WC, which is consistent with the temperature-induced changes in the PVD films of various phases of tungsten carbides [31]. According to our previous work on hydrazine decomposition [24], the metastable W_2C has an intrinsically higher activity than the thermally stable WC for hydrazine decomposition. Thus, we suggest that a possible reason for the slightly lower activity of the WC_x/AC-1123 catalyst is due to the formation of WC. Another possible reason is that a higher CHR temperature may lead to some sintering of WC_x particles, which decreases the number of active sites. Quite different from the high activity and selectivity of tungsten carbides, the Mo_2C/AC-973 catalyst showed a low selectivity to EG and other polyols, with the EG yield of only 5.3% (entry 5). The main products over the Mo_2C/AC-973 catalyst are unsaturated acids resulting from incomplete hydrolysis of cellulose. From the XRD result in Fig. 2, one can see that phase-pure Mo_2C has already been formed at the CHR temperature of 973 K, which is lowered by 100 K compared to W_2C.

The above results show that different catalysts performed very differently in converting cellulose to polyols. Since glucose has higher reactivity than hexitols, we propose that EG and other low-molecular weight polyols originate predominantly from the hydrogenolysis of glucose, while the sugar alcohols are resulting from the hydrogenation of glucose, as shown in Scheme 1. The high selectivity of EG on the W_2C/AC catalysts suggests that glucose hydrogenolysis prevails over its hydrogenation. On the contrary, an inverse case occurred on the Pt catalyst because Pt can dissociate H_2 more easily than tungsten carbides. It thus can be concluded that in the cellulose conversion reaction, tungsten carbides can be considered as a more efficient but low-cost catalyst to replace the precious metal catalyst for the production of EG.

Table 3
Surface areas and actual loadings of Ni in different catalysts determined by ICP analyses.

Catalyst	BET surface area (m^2/g)	Ni nominal loading (%)	Ni actual loading (%)
1%Ni-30%W_2C/AC-973	401	1	1.4
2%Ni-30%W_2C/AC-973	236	2	3. 8
3%Ni-30%W_2C/AC-973	199	3	6.1
30%W_2C/AC-1073	449	0	0.0

3.3. *Effect of the support type on the catalytic performance*

Not only the metal active phase but also the support itself exerted a great influence on the product distribution. For example, as shown in Table 1, when alumina was used as the support, either tungsten carbide or molybdenum carbide performed poorly in the polyol production (entries 7 and 8). In contrast, the Pt/Al_2O_3 (entry 6) gave a

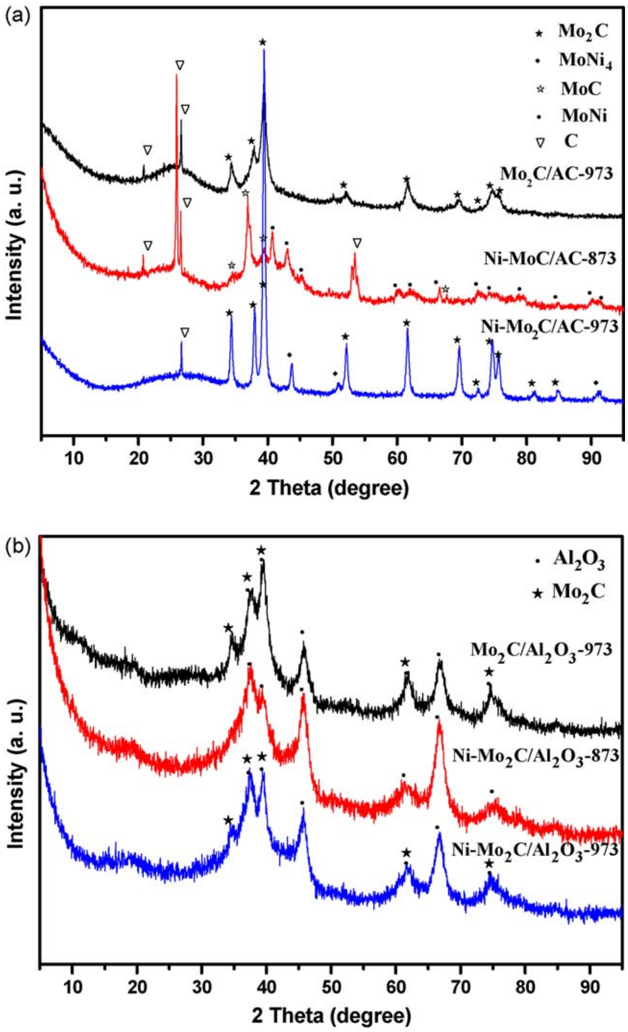

Fig. 7. XRD patterns of (a) AC-supported and (b) alumina-supported Mo_2C and Ni-promoted Mo_2C catalysts.

high conversion of cellulose (98%), and the EG yield was 14.2%. It is noted that the hexitol yield on the Pt/Al_2O_3 was even higher than the EG yield, reaching 15.5% (9.5% sorbitol and 6.0% mannitol). In addition, the yield of propylene glycol was also high, with a value of 9.3%. Evidently, the Pt/Al_2O_3 catalyst exhibited a much better performance than the Pt/AC, but the inverse case is observed for the carbide catalysts. Even for the carbon supported carbides, different carbon supports yielded different catalyst performance. Three types of carbon were considered in our work: active carbon (AC), carbon black (CB), and active carbon fibers (ACF). From Table 1 (entries 9 and 10), one can see that the W_2C/CB-1073 catalyst also performed well for the direct conversion of cellulose into EG, with the conversion of cellulose reaching 98% and the EG yield being 18.9%. However, the EG yield was still lower than that on the W_2C/AC-1073 (entry 3). On the other hand, the W_2C/ACF-1073 exhibited a very low yield of EG, suggesting that the ACF is not a good support for tungsten carbides for cellulose conversion.

Fig. 3 presents the XRD patterns of four different supported tungsten carbides. One can see that on the three carbon supports well-crystallized and phase-pure W_2C was formed. However, no crystalline phase of tungsten carbides was identified by XRD on the alumina support possibly due to the high dispersion of tungsten carbides on the support. The TEM images shown in Fig. 4 indicate that large (10–20 nm) W_2C particles are formed on both the AC and CB supports, while small particles with sizes less than 5 nm are highly dispersed on the alumina support. The dispersion of the various catalysts was measured by microcalorimetry of CO adsorption. As shown in Table 2, the dispersion of the catalysts increased in the sequence of W_2C/CB-1073 < W_2C/AC-1073 < W_2C/ACF-1073 < WC_x/Al_2O_3-1123. However, the trend in surface area does not correspond to the catalytic activity trend because of the different supports.

3.4. Promotional effect of Ni on the catalytic performance of carbides

From the above results we know that both Ni and carbides are active for the catalytic conversion of cellulose to polyols. Considering that tungsten carbides are particularly efficient for the selective formation of EG and Ni is a well known active catalyst for glucose hydrogenation [32], we synthesized bimetallic catalysts of Ni-W_2C to further enhance the EG yield. For comparison, Ni-Mo_2C was also prepared by a similar method.

From Table 1 (entries 11–21), one can see that with the promotion of Ni, the catalytic performances of W_2C and Mo_2C are significantly improved. Such a promotional effect is more pronounced on the W_2C/AC catalysts (entries 11–17). The highest EG yield, as high as 61.0%, was obtained on the 2%Ni-W_2C/AC-973 catalyst, along with a complete conversion of cellulose. Note that this value is much higher than the sum of EG yields on the W_2C/AC (entry 3) and Ni-AC (entry 2), indicating that there is a synergetic effect between Ni and W_2C in the reaction of cellulose degradation. Another feature of the Ni-W_2C/AC catalysts is the effect of CHR temperature. Although a higher CHR temperature led to a slight decrease of the EG yield over the W_2C/AC catalysts, it brought about a large decrease of the EG yield, from 61.0% to 39.2%, on the corresponding Ni-W_2C/AC catalyst (entries 12 and 15). The optimum nominal Ni loading on the W_2C/AC catalyst was found to be 2%. In contrast to Ni-W_2C, there is no synergistic effect on the Ni-Mo_2C catalyst, which shows an EG yield of only 11.3% (entry 18), which is similar to the sum of the yields on the Ni and Mo_2C catalysts.

Fig. 5a shows the XRD patterns of the Ni-W_2C catalysts that were prepared at different CHR temperatures. It can be seen that phase-pure W_2C was already formed at 973 K with the promotion of Ni, which is 100 K lower than unpromoted W_2C (compared with Fig. 2). According to literature [25], the formation of W_2C by the CHR method involves the progressive reduction of WO_3 to W and then to W_2C, which can be represented by the following overall reaction:

$$WO_x + C^* + H_2 \rightarrow W_2C + CO + H_2O$$

The presence of Ni can facilitate the reduction of WO_x by promoting the dissociation of H_2, resulting in the formation of W_2C at a lower temperature. Thus, it can be deduced that the Ni

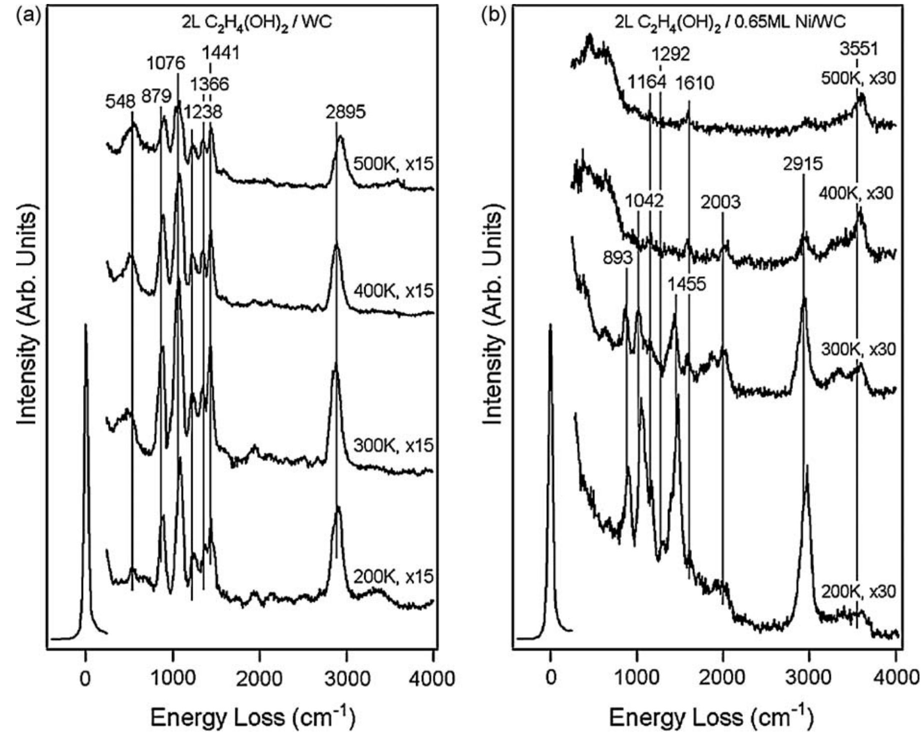

Fig. 8. Vibrational spectra recorded as a function of temperature of EG on WC and Ni-WC surfaces.

component must be in close contact with the WO_x species to facilitate H spillover from the Ni sites to WO_3 sites. These XRD results suggest the synergy between Ni and W_2C, in good agreement with the excellent performance of the Ni-W_2C catalyst in cellulose conversion.

On the other hand, it can be observed that with the elevation of the CHR temperature from 973 K to 1073 K, the XRD peaks of the W_2C became very sharp, both on the AC and alumina supports (Fig. 5), indicating that particle sintering is significant at this temperature. From the TEM images in Fig. 6, one can see that the presence of Ni significantly promoted the sintering of W_2C particles. Very large particles from tens to hundreds of nanometers are observed on the Ni-W_2C/AC-973 and Ni-W_2C/AC-1073 catalysts. The sintering of W_2C particles by the addition of Ni is most likely due to the fact that the presence of Ni accelerates the methanation of the carbon support. When the Ni-W_2C/AC catalyst precursor was treated in H_2 flow with a temperature-programmed reaction (TPR) mode, a very sharp peak of CH_4 ($m/e = 15$) appeared at ca. 800 K, which is lower by ca. 300 K than the unpromoted W_2C/AC catalyst. As a result of methanation of the carbon support, the actual Ni content of the 2%Ni-30%W_2C/AC-973 catalyst increased from the initial 2 wt%–3.8 wt% and the specific surface area decreased substantially from 449 m^2/g to 236 m^2/g (Table 3). The higher the Ni content, the more severe is the methanation extent. This can be explained by the continuing drop of the specific surface area with increasing the Ni content. Meanwhile, the actual W content is concomitantly increased, although the W content in the range of 30–60% did not influence the EG yield according to our previous study [13].

Different from the case of Ni-W_2C, the presence of Ni did not facilitate the formation of Mo_2C at a lower temperature. As shown in Fig. 7, regardless of the presence of Ni, well-crystallized and phase-pure Mo_2C was only formed above 973 K. When the CHR temperature was set as 873 K, only MoNi alloy phase was identified by XRD. This result implies that there is no synergy between Mo_2C and Ni, which is consistent with the activity tests in Table 1.

The above XRD and TEM results demonstrate that the addition of Ni to the W_2C/AC catalyst facilitates the formation of the W_2C phase at a lower temperature. On the other hand, it also induces significant sintering of W_2C particles. The remarkably enhanced activity and selectivity to EG may be ascribed to the synergistic effect between Ni and W_2C, as well as to the increased Ni and W content by the methanation of the carbon support.

3.5. Surface science studies of EG on WC and Ni-WC

In order to further understand the modification effect of Ni, fundamental surface science studies were performed following the adsorption of EG on well characterized WC and 0.65 ML (monolayer) Ni-WC surfaces. As shown in Fig. 8a, the HREEL spectrum on WC at 200 K shows vibrational features that are characteristic of EG based on a recent study [33]. The vibrational features include $\rho_r(CH_2)$ at 879 cm^{-1}, $\nu_s(CO)$ at 1076 cm^{-1}, $\rho_t(CH_2)$ 1238 cm^{-1}, $\rho_w(CH_2)$ at 1366 cm^{-1}, $\delta(CH_2)$ at 1441 cm^{-1}, $\nu_{as}(CH)$ at 2895 cm^{-1}, and a broad $\nu(OH)$ mode at $\sim$3300 cm^{-1}. At higher temperatures, the $\nu(OH)$ mode disappears while the other vibrational features retain the same frequencies, due to the formation of the ethylenedioxy intermediate ($-OCH_2CH_2O-$) as recently observed on the Pt(1 1 1) [33]. These vibrational features remain on the surface even after heating to 500 K, indicating that the ($-OCH_2CH_2O-$) species adsorb strongly on the WC surface.

In contrast, on the Ni-WC surface (Fig. 8b) the vibrational features of EG appear at slightly different frequencies and with different relative intensities, suggesting that the presence of Ni significantly modifies the bonding configuration of EG on WC. More importantly, after heating to 400 K all EG features between 893 cm^{-1} and 1455 cm^{-1} disappear, most likely due to the desorption of EG from the Ni-WC surface. The feature at 3551 cm^{-1} is not related to EG and is from the OH groups produced from the interaction of H_2O in the UHV background with Ni-WC. The comparison of spectra in Fig. 8 reveals that the presence of low coverage of Ni reduces the bonding between EG and WC, which should in turn prevent the further decomposition of EG or ($-OCH_2CH_2O-$) on Ni-WC. This observation is consistent with the reactor studies of higher EG yield on Ni-promoted tungsten carbides as shown in Table 1.

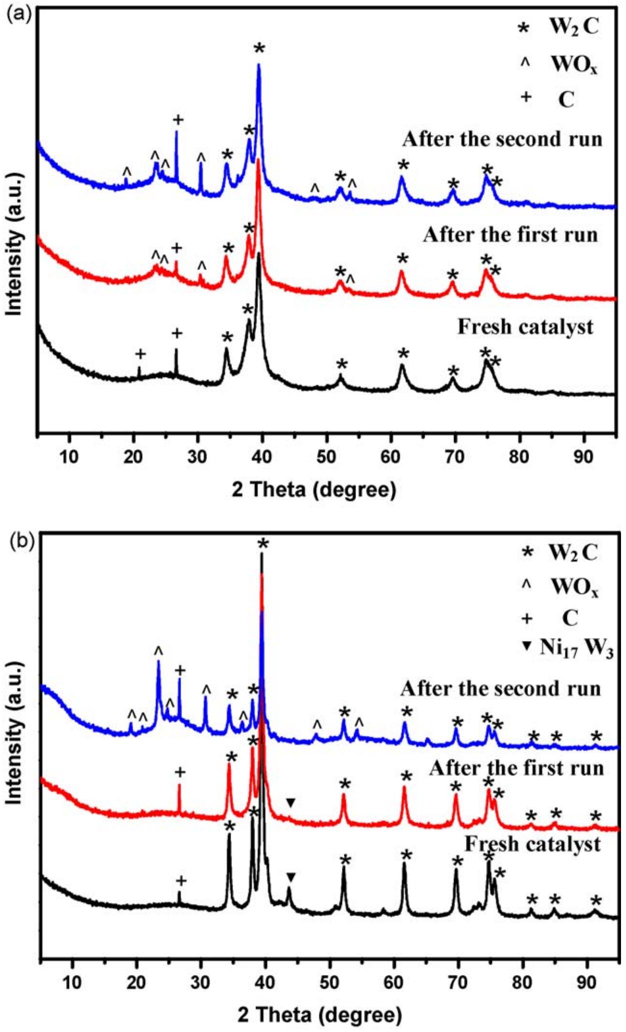

Fig. 9. XRD patterns of (a) W_2C/AC-1073 and (b) 2%Ni-W_2C/AC-973 catalysts before and after the reaction.

As reported in our previous studies [31,34], the formation of phase-pure W_2C and WC surfaces depends on the synthesis conditions, such as the reaction environment and temperatures. Under the conditions used in the current surface science work the WC surface was preferred. Studies are underway to synthesize Ni-W_2C for additional surface science studies. Nevertheless, the results in Fig. 8 clearly indicate that the presence of Ni on tungsten carbides reduces the activity toward the decomposition of ethylene glycol.

3.6. Reusability of the catalysts

The ability for recycling is always important for metal-catalyzed liquid-phase reactions. Therefore, we recycled W_2C/

AC-1073 and 2%Ni-W_2C/AC-973 catalysts over three runs. From Table 1, one can see that the yield of EG over the W_2C/AC-1073 catalyst slightly decreased from 27.4% to 23.6% in the second run, and remained nearly constant in the third run (entries 22 and 23). Similarly, the Ni-W_2C/AC-973 catalyst also exhibited a slight loss in EG yield during the second and third run (entries 24 and 25). To reveal the reason for the slight drop in repeated runs, we performed the ICP analysis of the liquid product to determine if W or Ni was leached from the catalyst during the reaction. The results show that the Ni and W concentrations of the liquid product after the first run were 2.7 ppm and 16.2 ppm, respectively; while they increased to 9.2 ppm and 51.9 ppm after the third run. The observation of the relatively low concentrations of Ni and W indicates that the leaching of metals is negligible, and it should not be considered as a major reason for the yield loss of EG during recycling. Instead, the XRD examinations (shown in Fig. 9) demonstrate that the active W_2C phase on the after-run catalyst has been slightly oxidized, which may be responsible for the slight loss of the EG yield during the recycling.

4. Conclusions

Supported carbide catalysts were synthesized and evaluated for the catalytic conversion of cellulose toward polyols, especially EG. These catalysts showed considerable activities for the conversion of cellulose. Among all the catalysts, 2%Ni-promoted W_2C/AC had the best catalytic activity, with the EG yield being as high as 61%. The corresponding surface science studies indicate that the enhanced EG yield is at least partially due to weaker bonding between EG and Ni-promoted tungsten carbides. In view of the importance of EG in petrochemical industry, our approach may open a new route for the production of chemicals directly from biomass. Furthermore, the utilization of carbide catalysts represents new opportunities for cellulose conversion by a heterogeneous catalytic process with less expensive catalysts.

Acknowledgements

Support of National Science Foundation of China (NSFC) for Distinguished Young Scholars (No. 20325620) is gratefully acknowledged. Authors from the University of Delaware acknowledge support from the United States Department of Energy (DE-FG02-00ER15104). We also thank Prof. Guowang Xu and Ms. Jing Chen for their help in HPLC–MS analysis.

References

[1] D.L. Klass, Biomass for Renewable Energy, Fuels and Chemicals, Academic Press, San Diego, 1998.
[2] G.W. Huber, S. Iborra, A. Corma, Chem. Rev. 106 (2006) 4044.
[3] L.R. Lynd, C.E. Wyman, T.U. Gerngross, Biocommodity engineering, Biotechnol. Prog. 15 (1999) 777.
[4] L.R. Lynd, P.J. Weimer, Microbiol. Mol. Biol. Rev. 66 (2002) 506.
[5] S.D. Mansfield, C. Mooney, J.N. Saddler, Biotechnol. Prog. 15 (1999) 804.
[6] A. Pizzi, N. Eaton, J. Macromol. Sci. Chem. 22 (1985) 105.
[7] Y.P. Zhang, L.R. Lynd, Biotechnol. Bioeng. 88 (2004) 797.
[8] W.S. Mok, M.J. Antal, G. Varhergyi, Ind. Eng. Chem. Res. 31 (1992) 94.
[9] M. Ishida, K. Otsuka, S. Takenaka, I. Yamanaka, J. Chem. Technol. Biotechnol. 80 (2005) 281.
[10] M. Sasaki, Z. Fang, Y. Fukushima, T. Adschiri, K. Arai, Ind. Eng. Chem. Res. 39 (2000) 2883.
[11] A. Fukuoka, P.L. Dhepe, Angew. Chem. 118 (2006) 5285–5287 (Angew. Chem. Int. Ed., 45 (2006) 5161).
[12] C. Luo, S. Wang, H.C. Liu, Angew. Chem. 119 (2007) 7780–7783 (Angew. Chem. Int. Ed., 46 (2007) 7636).
[13] N. Ji, T. Zhang, M.Y. Zheng, A.Q. Wang, H. Wang, X.D. Wang, J.G. Chen, Angew. Chem. Int. Ed 47 (2008) 8510.
[14] R. Levy, M. Boudart, Science 181 (1973) 547.
[15] S.T. Oyama, Catal. Today 15 (1992) 179.
[16] H.H. Hwu, J.G. Chen, Chem. Rev. 105 (2005) 185.
[17] B. Fruhberger, J.G. Chen, J. Am. Chem. Soc. 118 (1996) 11599.
[18] N. Liu, S.A. Rykov, J.G. Chen, Surf. Sci. 487 (2001) 107.
[19] P. Liu, J.A. Rodriguez, J. Chem. Phys. 120 (2004) 5414.
[20] R. Barthos, F. Solymosi, J. Catal. 249 (2007) 289.
[21] X.W. Chen, T. Zhang, P.L. Ying, M.Y. Zheng, W.C. Wu, L.G. Xia, Can. Li, X.D. Wang, Can. Li Chem. Commun. (2002) 288.
[22] R.H. Cheng, Y.Y. Shu, M.Y. Zheng, L. Li, J. Sun, X.D. Wang, T. Zhang, J. Catal. 249 (2007) 397.
[23] ICIS Chemical Business (Weekly), 352 (2008) July 28.
[24] J. Sun, M.Y. Zheng, X.D. Wang, A.Q. Wang, R.H. Cheng, T. Li, T. Zhang, Catal. Lett. 123 (2008) 150.
[25] C.H. Liang, F.P. Tian, Z.L. Li, Z.C. Feng, Z.B. Wei, C. Li, Chem. Mater. 15 (2003) 4846.
[26] L. Li, X. Wang, X.D. Wang, X.Q. Zhao, M.Y. Zheng, R.H. Cheng, L.X. Zhou, T. Zhang, Thermochim. Acta. 434 (2005) 119.
[27] N. Liu, K. Kourtakis, J.C. Figueroa, J.G. Chen, J. Catal. 215 (2003) 254.
[28] E.C. Weigert, A.L. Stottlemyer, M.B. Zellner, J.G. Chen, J. Phys. Chem. C 111 (2007) 14617.
[29] L.E. Murillo, A.M. Goda, J.G. Chen, J. Am. Chem. Soc. 129 (2007) 7101.
[30] W. Lee, N.A. DaSilva, Metab. Eng. 8 (2008) 58.
[31] E.C. Weigert, M.P. Humbert, Z.J. Mellinger, Q. Ren, T.P. Beebe Jr., L. Bao, J.G. Chen, J. Vac. Sci. Technol. A26 (2008) 23.
[32] P. Gallezot, P.J. Cerino, B. Blanc, G. Fleche, P. Fleche, J. Catal. 146 (1994) 93.
[33] O. Skoplyak, M.A. Barteau, J.G. Chen, Surf. Sci 602 (2008) 3578.
[34] M.B. Zellner, J.G. Chen, Catal. Today 99 (2005) 299.